

CHEMISTRY

A European Journal

A Journal of



Accepted Article

Title: A Bifunctional Fluorogenic Rhodamine Probe for Proximity-Induced Bioorthogonal Chemistry

Authors: Philipp Werther, Jasper S. Möhler, and Richard Wombacher

This manuscript has been accepted after peer review and appears as an Accepted Article online prior to editing, proofing, and formal publication of the final Version of Record (VoR). This work is currently citable by using the Digital Object Identifier (DOI) given below. The VoR will be published online in Early View as soon as possible and may be different to this Accepted Article as a result of editing. Readers should obtain the VoR from the journal website shown below when it is published to ensure accuracy of information. The authors are responsible for the content of this Accepted Article.

To be cited as: *Chem. Eur. J.* 10.1002/chem.201703607

Link to VoR: <http://dx.doi.org/10.1002/chem.201703607>

Supported by
ACES

WILEY-VCH

A Bifunctional Fluorogenic Rhodamine Probe for Proximity-Induced Bioorthogonal Chemistry

M.Sc. Philipp Werther[‡], M.Sc. Jasper S. Möhler[‡] and Dr. Richard Wombacher*

Institut für Pharmazie und Molekulare Biotechnologie, Ruprecht-Karls-Universität Heidelberg, Im Neuenheimer Feld 364, 69120 Heidelberg, Germany.

E-mail: wombacher@uni-heidelberg.de

[‡] These authors contributed equally

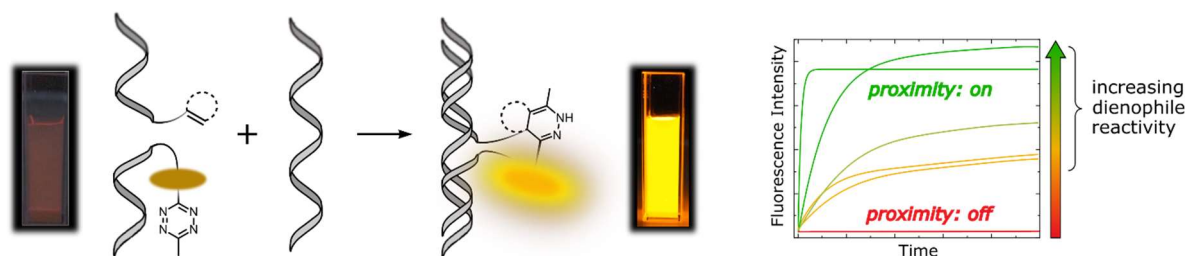
*Corresponding author

Accepted Manuscript

Abstract

Bioorthogonal reactions have emerged as a versatile tool in life sciences. The inverse electron demand Diels-Alder reaction (DA_{inv}) stands out due to the availability of reactants with very fast kinetics. However, highly reactive dienophiles suffer the disadvantage of being less stable and prone to side reactions. Here, we evaluate the extent of acceleration of rather unreactive but highly stable dienophiles by DNA-templated proximity. To this end, we developed a modular synthetic route for a novel bifunctional fluorogenic tetrazine rhodamine probe that we used to determine the reaction kinetics of various dienophiles in a fluorescence assay. Under proximity-driven conditions the reaction was found to be several orders of magnitude faster, and we observed almost no background reaction when proximity was not induced. This fundamental study identifies a minimally sized fluorogenic tetrazine dienophile reactant pair that has potential to be generally used for the visualization of biomolecular interactions with temporal and spatial resolution in living systems.

Graphical Abstract



Introduction

One of the most important criteria in the synthesis of complex organic molecules is “chemoselectivity”, a term first coined by Barry M. Trost in 1973^[1]. IUPAC^[2] defines chemoselectivity as the “preferential reaction of a chemical reagent with one of two or more different functional groups”. In the more recent past, chemists have started to perform chemical reactions in biological environments for labeling purposes, to modify or to control the function of biomolecules. Once more, this challenges researchers to solve even more sophisticated problems of chemoselectivity: In the overcrowded and dense cellular milieu, a multitude of endogenous molecules carrying a vast number of chemical functionalities, small nucleophilic molecules, (metal) ions, reactive oxygen species etc. are present and potentially interfere with introduced artificial chemistry. Reactions that exhibit satisfying chemoselectivity in biosystems have been termed “bioorthogonal” by Carolyn R. Bertozzi in 2003.^[3] To truly accomplish a bioorthogonal reaction, additional requirements have to be fulfilled. Starting material, product, by-products should not be harmful to the biological system and must not interfere with cellular or tissue processes. Moreover, the formed inert chemical bond must not perturb native biomolecule function in an unwanted way. Another crucial aspect is the kinetic profile of the reaction: The reaction must be reasonably fast in the aqueous milieu (physiological pH, high salt content, reactive nucleophiles) of biological systems.^[4] Several reactions that match these criteria have been (re-)invented by chemical biologists. These include the Staudinger ligation^[5] and the catalyst-free strain-promoted azide alkyne cycloaddition (SPAAC)^[6] as well as the inverse electron demand Diels-Alder cycloaddition between 1,2,4,5-tetrazines and (strained) olefins (DA_{inv}).^[7]

Based on superior characteristics, DA_{inv} has emerged as bioorthogonal chemistry of choice in many applications.^[8] Contrary to normal electron demand Diels-Alder reactions, DA_{inv} employs weak Michael acceptors as dienophiles which are rather stable against endogenous nucleophiles. Moreover, the release of dinitrogen as the only by-product drives the equilibrium. The outstanding advantage of the DA_{inv} is its extremely fast kinetics (k_2 up to $10^6 \text{ M}^{-1}\text{s}^{-1}$ ^[9]) As a fortunate circumstance, aqueous reaction media increase rates compared to other protic (and aprotic) solvents.^[10] Rapid reactions are crucial if fast cellular processes are under investigation and to diminish competing slower side reactions. The fastest known rates in bioorthogonal chemistry have been achieved with ring-strained olefins in DA_{inv}. However, despite of its popularity in recent applications for biomolecular modification,

limitations have emerged on using this chemistry. High reactivity in chemistry comes with the cost of selectivity, as reactive species are less stable and therefore open to alternate reaction pathways. This has come to display in DA_{inv} as well. Broadly used *trans*-cyclooctenes (TCOs) are prone to isomerize to less reactive *cis*-cyclooctenes.^[11] Other dienophiles undergo elimination post-cycloaddition^[12] and (electron-deficient) tetrazines can react with endogenous nucleophiles.^[13] If DA_{inv} is applied in protein labeling, this leads to a low labeling density, which is a drawback for biophysical applications like localization microscopy. Although numerous interesting approaches aim to stabilize TCOs by structural modification,^[9, 14] it is highly challenging to maintain high reactivity at the same time. Taken altogether, the key feature of DA_{inv} , the rapid reaction rates, potentially puts the bioorthogonality requirement “chemoselectivity” at risk. One way to overcome this stalemate situation is the use of stable and less reactive DA_{inv} -reactants in combination with a secondary, proximity-inducing process that accelerates reaction rates.

In the concept of proximity-induced rate enhancement, molecular recognition creates an intramolecular situation and therefore increases the active concentrations of the reactants and hence the overall rate of the reaction. Proximity-accelerated reactions are not only of prime interest in the design of improved bioorthogonal reactions, but have been used extensively for sensing and imaging of nucleic acids.^[15] Staudinger ligation^[16] (e.g. QSTAR probes), copper catalyzed azide alkyne cycloaddition (CuAAC),^[17] native chemical ligation,^[18] nucleophilic substitution (S_N)^[19] as well as photoligation^[20] are notable chemistries templated by nucleic acids. Two recent publications that utilize templated turn-over reactions elucidate the advancement this field has come to already: Kool *et al.* used Staudinger chemistry to detect RNA at concentrations of 10 pM and single point deletions while the Winssinger group reached enzyme-like rates in the PNA-templated photocatalytic reduction of azides.^[21] Beyond that, ligand-directed reactions are of special interest for the development of covalent drugs^[22] and in protein labeling schemes^[23]. Oligonucleotide-mediated DA_{inv} have been developed by the Devaraj group for the reaction turn-over sensing of mRNA.^[24] They employed a tetrazine fluorogenic BODIPY dye and vinyl-ether-caged cyanine fluorophore, both inducing strong fluorescence after undergoing DA_{inv} and enabling a reaction turnover (Figure 1).

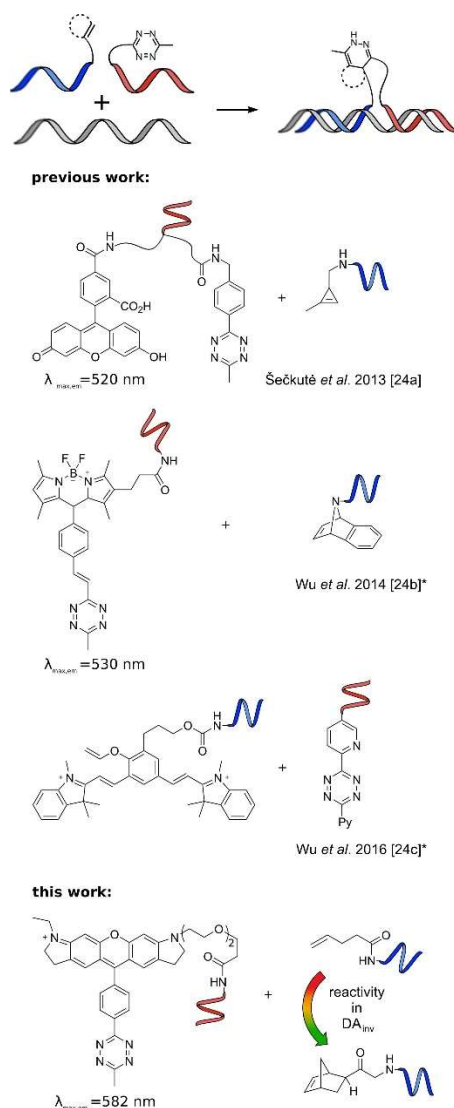


Figure 1: Schematic overview of templated chemistry using dienophiles and tetrazine fluorophore conjugates or dienophile-caged fluorophores respectively. *References marked with asterisks report initial template-mediated cycloadditions, followed by elimination resulting in reaction turnover.

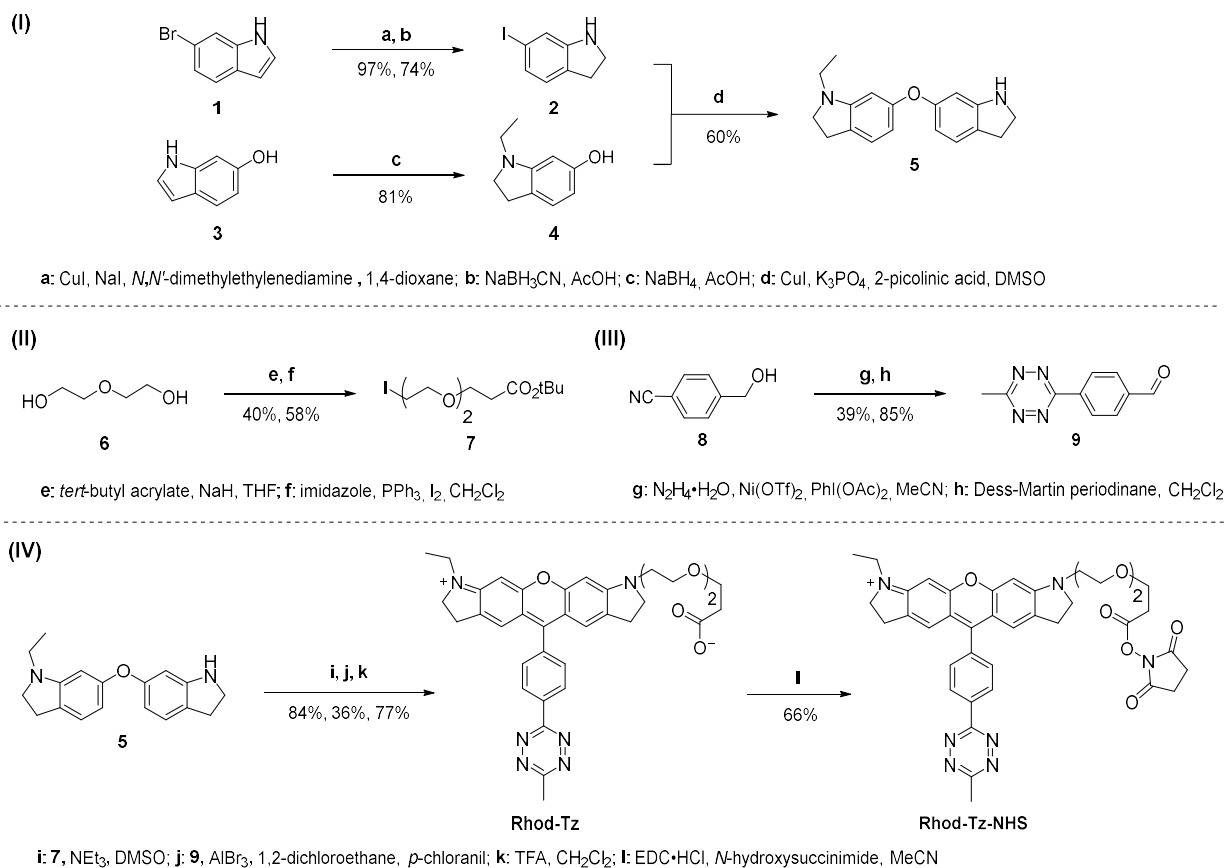
In the light of the overall relevance of proximity-induced chemistry in life sciences and in particular of the significance and current limitations of DA_{inv} for bioorthogonal chemistry, it is of special interest to evaluate the scope of DA_{inv} in proximity-induced chemistry. To this end, we present the design and synthesis of a highly fluorogenic tetrazine rhodamine probe that is equipped with an additional functionality for further conjugation to biomolecules. The novel dye was ideally suited to study the rate-acceleration of rather unreactive and stable dienophiles in nucleic acid-templated DA_{inv} with a direct and sensitive fluorescence read-out. This work represents a comprehensive evaluation of dienophile-reactivity under non-mediated and template-mediated conditions and gives valuable information and indications for future developments of highly bioorthogonal reactions. Moreover, the presented

fluorogenic tetrazine rhodamine dye equipped with a biomolecule targeting site is predestined for advanced studies of biological processes.

Results and Discussion

Modular Synthesis of a Bifunctional Tetrazine Rhodamine

To investigate proximity-directed DA_{inv} with a fluorogenic tetrazine reporter, we envisioned a synthetic strategy based on recent work from our laboratory. In this approach, tetrazinyl benzaldehydes were reacted with diarylethers (or silanes) in Friedel-Crafts reactions to assemble fluorogenic tetrazine (Si)rhodamines which we showed to be suitable for no-wash protein labeling inside living cells.^[25] The design of the fluorophore probe followed the principles: (1) minimal interchromophore distance between the fluorophore and the tetrazine for strong fluorescence quenching and for small probe size, (2) well-suited fluorophore classes for biological application (3) modular synthetic access under mild conditions. Due to the modular nature of our strategy, a biarylether can alternatively be used in the Friedel-Crafts reaction as nucleophile that carries an additional carboxylic function for bioconjugation. The convergent synthesis route (Scheme 1) opens the door to easily accessible fluorogenic tetrazine rhodamine dyes that can be conjugated to a biomolecule with an intact tetrazine moiety still efficiently quenching the fluorophore. Subsequently, the tetrazine can be used for a second conjugation by DA_{inv} resulting in a strong increase of fluorescence, equivalent to a small molecule-based “light-up” cross linker. In this work, a novel bifunctional reporter (**Rhod-Tz-NHS**) was used to investigate a set of different dienophiles of various reactivity in proximity-accelerated DA_{inv}. For the synthesis of **Rhod-Tz-NHS**, biarylether **5** was obtained *via* a Cu^I-mediated coupling reaction of aryl iodide **2** with phenol **4** in 60% yield (Scheme 1, I).^[26] Precursors **2** and **4** were obtained from the commercially available starting materials **1** and **3** by either halogen exchange reaction with subsequent reduction (for **2**) or simultaneous reduction and ethylation (for **4**).^[26a, 27] Diethylene glycol was converted to **7** over two steps^[28] resulting in a PEG-2 chain linker that enhances hydrophilicity of the final fluorogenic probe. To be compatible with Lewis acid-mediated Friedel-Crafts reaction, the carboxylic acid was *tert*-butyl ester-protected (Scheme 1, II). Tetrazine benzylic alcohol was afforded from hydroxymethyl benzonitrile (39%) and subsequently oxidized to benzaldehyde **9** using Dess-Martin periodinane (85%) (Scheme 1, III).^[25]



Scheme 1: Three building blocks (I-III) enable the modular synthesis (IV) of the bifunctional dye **Rhod-Tz-NHS**.

After attaching **7** to the biarylether **5** (84%), the resulting modified biarylether was converted with benzaldehyde **9** to tetrazinyl rhodamine **S5** via AlBr₃-mediated Friedel-Crafts reaction and subsequent oxidation with *p*-chloranil (36%). Deprotection of **S5** yielded **Rhod-Tz** in 77% yield. **Rhod-Tz-NHS** was obtained by using a standard protocol (EDC·HCl, *N*-hydroxysuccinimide) and subsequent HPLC purification yielded the target fluorogenic probe in the purity needed for further experiments (66%) (Scheme 1, IV). We would like to highlight particularly that the modular nature of the herein developed route (building blocks I-III in Scheme 1) allows the independent modification of each building block providing the synthetic flexibility needed for further tailor-made probes. To the best of our knowledge, **Rhod-Tz-NHS** represents the first fluorogenic tetrazine crosslinker based on a rhodamine fluorophore. First, the probe can be conjugated to an amine of a biomolecule, presenting the tetrazine for a second fluorogenic bioorthogonal DA_{inv}.

Photophysical Characterization of the Bifunctional Probe

Overall, the herein described synthesis represents a novel access to a highly water-soluble fluorogenic probe which carries two orthogonal reactive groups for bioconjugation. Most

importantly, the tetrazine fluorophore probe exhibits strong fluorescence enhancements upon conversion in DA_{inv} (Figure 2a). Before applying the novel tetrazine probe in the investigation of proximity-accelerated DA_{inv}, we first evaluated its photophysical and fluorogenic properties (Figure 2b-d). Absorption and emission spectra of **Rhod-Tz** were recorded in aqueous phosphate buffered saline (PBS) and the absorption maximum was determined to $\lambda_{\text{abs}} = 559 \text{ nm}$ ($\epsilon = 4.4 \cdot 10^4 \text{ M}^{-1} \text{ cm}^{-1}$), the emission maximum to $\lambda_{\text{em}} = 582 \text{ nm}$ (Figure 2b). The fluorescence quantum yield $\Phi_f = 0.017$ is in accordance with previously reported tetrazine quenched rhodamines.^[25]

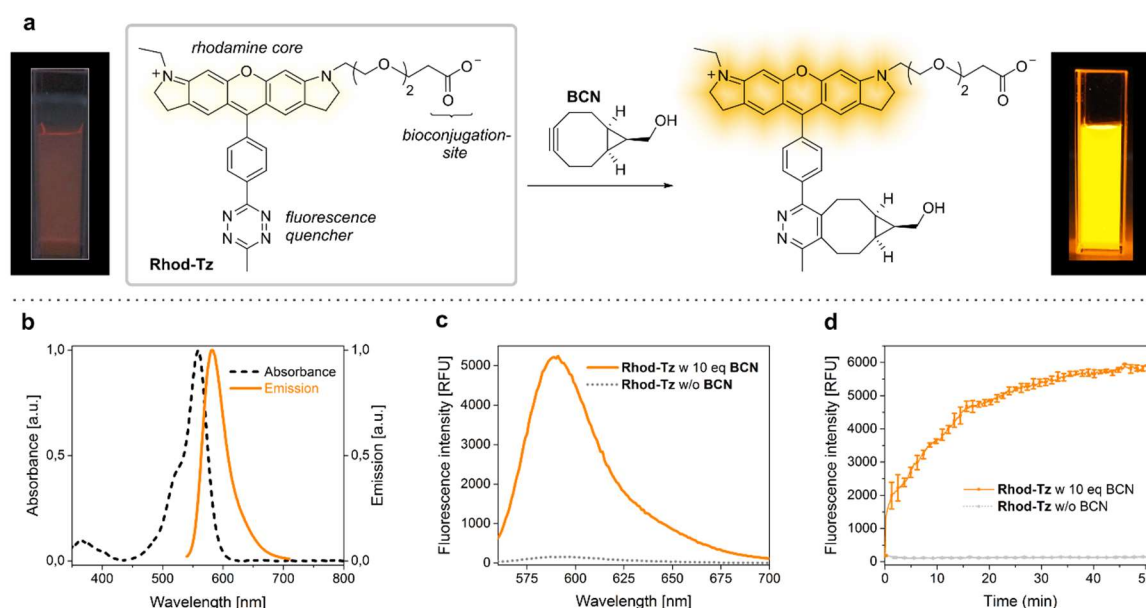


Figure 2: Photophysical properties and fluorogenicity of Rhod-Tz. (a) Reaction with BCN. Cuvettes with Rhod-Tz were irradiated with a handheld UV-lamp (365 nm) w (left) and w/o (right) BCN. (b) Normalized absorption and emission spectra. (c) Emission spectra w/o BCN and after addition of 10 eq BCN. (d) Time course measurement. (a: 10 μM , b-c: 1 μM , each in PBS).

Fluorogenicity of **Rhod-Tz** was quantified to 34-fold fluorescence enhancement when converted with (1R,8S,9s)-bicyclo[6.1.0]non-4-yn-9-ylmethanol (BCN) as model dienophile. Ten equivalents of BCN led to completion of fluorescent product formation after 40 minutes (Figure 2d). This “turn-on factor” is slightly improved, compared to recently published fluorogenic tetrazine rhodamines with ultra-short interchromophore distance (1.6 fold higher).^[25] Furthermore, the water-soluble dye is highly stable in aqueous buffer at room temperature and no degradation was observed over 12 hours. The fluorescence quenching efficiency is in general dependent on the interchromophore distance and a number of short-distance tetrazine fluorophore conjugates have been reported.^[25, 29] The exact quenching

mechanism for these fluorogenic tetrazine probes is still under debate, as no thorough physicochemical investigation has been reported yet.

Dienophiles for Proximity-Induced DA_{inv}

Various dienophile classes have found widespread application in bioorthogonal reactions with tetrazines in DA_{inv} . These range from unstrained and slowly reacting primary olefins^[30] to ring-strained and more reactive dienophiles such as norbornenes^[7b] and cyclopropenes.^[31] Highly strained cyclic alkynes (e.g. cyclooctynes, e.g. BCN) and olefins (prominently *trans*-cyclooctenes, e.g. TCO, sTCO) are among the dienophiles reaching the fastest reaction kinetics. Due to the extremely rapid reaction rates, especially TCO-derivatives have emerged to dienophiles of choice in DA_{inv} ($k_2 \leq 10^6 \text{ M}^{-1} \text{ s}^{-1}$ in aqueous media^[9]). However, their applicability is constrained to a certain degree as they degrade under prolonged storage and thiol exposure leads to metabolic instability under serum conditions.^[9, 11a] In this context, tremendous efforts have been made to develop stable and still highly-reactive TCO-dienophiles.^[9, 14] Moreover, the rather large size of TCOs may perturb native biomolecule function and the hydrophobicity of TCO-derivatives has been linked to increased fluorescent background in imaging and the necessity of elaborate washing procedures.^[14f, 32] Bypassing TCO-derivatives entirely, an obvious approach would be to use less reactive, smaller and more stabilized dienophiles. Their intrinsic slow reaction rates in DA_{inv} can be overcome by inducing spatial proximity between the reactants. A promising model system for proximity-acceleration, as has been shown by the Devaraj group for DA_{inv} ,^[24a] is the molecular recognition of nucleic acid hybrids. DNA-templated chemistry was also chosen in this study to evaluate the extent of proximity-acceleration on dienophiles of varying reactivity.

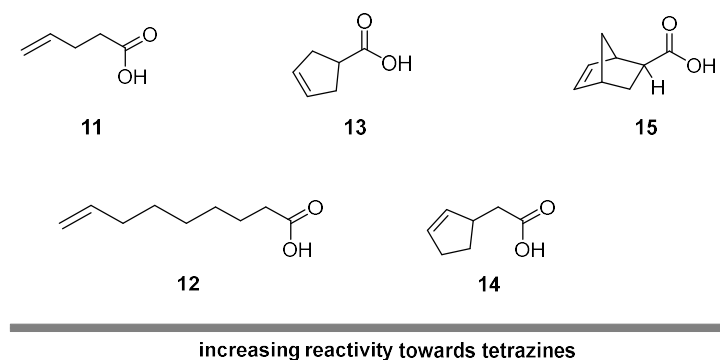


Figure 3: Dienophiles with a broad spectrum of reactivity in DA_{inv} and high stability in biological environments.

To this end, we selected a set of stable dienophiles ranging from low to medium reactivity which react rapidly only under proximity-driven conditions (Figure 3). These include unstrained linear α -olefins ($k_2 \sim 10^{-2} \text{ M}^{-1} \text{ s}^{-1}$,^[30a, 30b] **11, 12**), cyclopentene (**13, 14**) and norbornene derivatives ($k_2 \sim 1.9 \text{ M}^{-1} \text{ s}^{-1}$ ^[7b], **15**), all of which exhibit reaction rates at least six orders of magnitude lower than TCO-derivatives. In particular, the accelerated reaction of slow α -olefin tags is of interest due to their minimal size and high stability.^[30c] Beyond the varying reactivity of the chosen dienophiles (Figure 3), our selection enables to study the effects of conformational freedom which supposedly has a profound influence on DA_{inv} -reactivity under proximity-mediated conditions. On this account, different linker lengths were chosen at the examples of primary alkenes (**11, 12**) and cyclopentene derivatives (**13, 14**). The commercially available unsaturated organic acids (**11 to 15**) were converted to their NHS-esters, (see SI) which can be used to attain dienophile-modified nucleic acids needed for template-driven DA_{inv} .

Conjugation of the Fluorogenic Diene and Dienophiles to DNA

The concept of proximity-driven DA_{inv} obviously carries the potential to put the reaction under control of a biomolecular interaction. Therefore, the dienophiles of choice should only react with the tetrazine (fluorogenic **Rhod-Tz**) when brought in close proximity. With the herein reported conjugatable fluorogenic tetrazine the biomolecular interaction can be translated into a fluorescent read-out signal. DNA hybridization is the most well-defined and previously extensively applied biomolecular interaction to create molecular proximity. Briefly, we studied the effect of proximity on DA_{inv} by using three components: (1) a 14mer oligonucleotide 3'-modified with the fluorogenic **Rhod-Tz**, (2) 14mer 5'-modified dienophiles and (3) various template sequences to examine the effects of sequence variation and length (Figure 4a-c). To

yield components (1) and (2), **Rhod-Tz-NHS** and the dienophiles (**11** to **15-NHS**, SI) were attached to the 3' or 5'-amino-modified oligonucleotides by means of amide coupling chemistry. We used flexible linker structures (Figure S1) between the amine functionalities and the 14mers to ensure the necessary conformational flexibility for the templated DA_{inv}. A ten to thirty-fold excess of the NHS-activated dienophiles or **Rhod-Tz-NHS** respectively was used to reach complete conversion of the amino-modified 14mers within two to four hours. The reaction mixtures were monitored by HPLC, subsequently purified on a preparative scale and the identity of the afforded 14mer-dienophiles and 14mer-Rhod-Tz was confirmed via LCMS (Table S1, Figure S1).

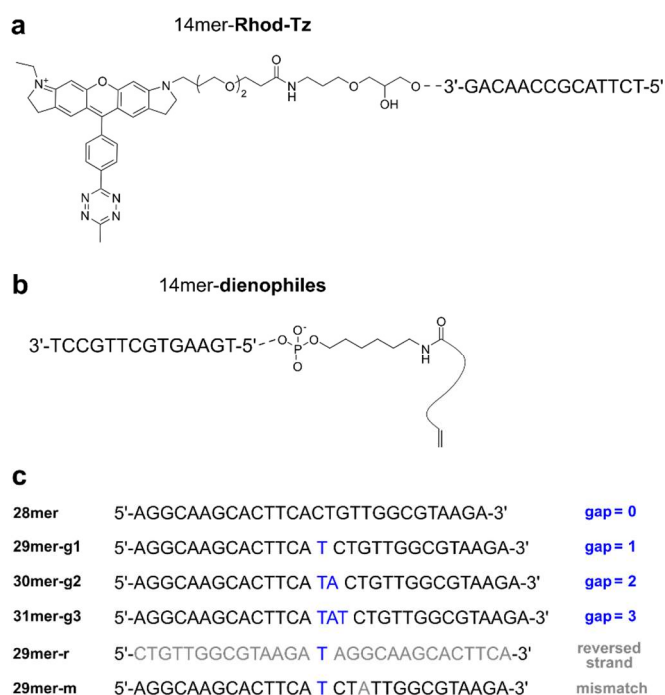


Figure 4: Components for proximity-accelerated DA_{inv}. Structure of 14mer-Rhod-Tz (a) and 14mer-dienophiles (b). (c) Varying template sequences to study the influence of base gaps between the DA_{inv}-reactants (28mer to 31mer-g3), of spatial separation through hybridization (29mer-r) or of a mismatch three bases apart from DA_{inv} reaction site (29mer-m).

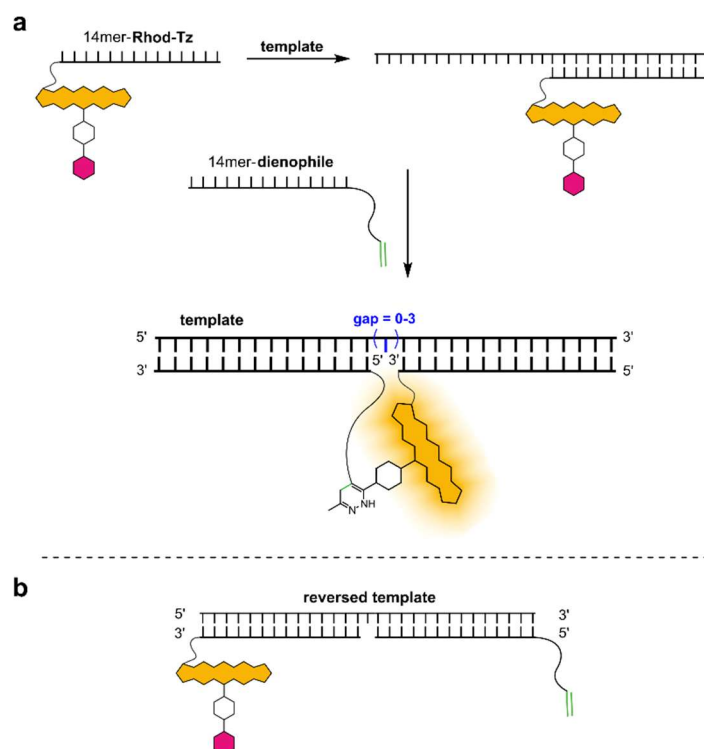


Figure 5: (a) Schematic representation of the assay: 14mer-**Rhod-Tz**, 14mer-**dienophiles**, template sequence and resulting cycloaddition product. (b) Reversed template places reactive groups on opposite ends of the formed hybrid (29mer-r).

Complementary template sequences were designed to hybridize with 14mer-**dienophile** and 14mer-**Rhod-Tz**. The exact template sequences are shown in Figure 4c. Templates 28mer, 29mer-**g1**, 30mer-**g2** and 31mer-**g3** were used to study the effect of varying distances between DA_{inv} -reactants. Moreover, a template with a reversed sequence (29mer-r) serves as a control where hybridization places the reactive groups on opposite ends of the double strand and thus prevents successful product formation. A randomly inserted mismatch in 29mer-**g1** provided the template 29mer-**m** which can be used to study the effect of imperfect hybridization on the proximity-enhanced reaction.

Rate Enhancement of DA_{inv} by Template-Induced Proximity

To study the influence of template-induced proximity on the reaction rates of different dienophiles in DA_{inv} , the above described tetrazine and dienophile-modified oligonucleotides were mixed in absence and presence of an oligonucleotide template strand at equimolar concentrations (1 μM) in aqueous PBS. The fluorogenic tetrazine allows to easily follow the reaction progress by recording the changes in fluorescence over time. To that purpose, the template DNA-strand was added to the fluorogenic probe-modified oligonucleotide 14mer-**Rhod-Tz** and the measurements were started upon addition of the dienophile-modified oligonucleotides 14mer-**dienophiles** (Figure 5a). Fluorescence intensity was

recorded every 45-135 s (depending on the speed of the reaction) over a total of four hours (excitation wavelength $\lambda_{\text{ex}} = 559$ nm, emission wavelength $\lambda_{\text{em}} = 582$ nm). To exclude that photo bleaching affects the measurements, we analyzed a control sample containing solely 14mer-**Rhod-Tz** in PBS with the same fluorometer settings. No significant changes in intensity could be observed over the entire experiment. The diagrams in Figure 6a-e show the reaction kinetics of the different 14mer-**dienophiles** with 14mer-**Rhod-Tz** in DA_{inv} in the presence of different templates. The template sequences were designed to be complementary to both 14mer sequences with either no or up to three additional bases in between (see Figures 4c and 5a). We supposed that, upon hybridization, the resulting gaps (g1, g2, g3) in the final double strand would position the dienophile and tetrazine at various distances and orientations, thereby creating different spatial proximity.

Whereas we did not observe any reaction in the absence of template over the entire period of four hours for 14mer-**11** to **14**, we did observe a slight increase in fluorescence when using the 14mer-**15** (Figure S2). From the change in fluorescence the consumption of 14mer-**15** in DA_{inv} can be calculated to below 0.6%. This indicates that even norbornene, the most reactive dienophile of this study, exhibits only negligible background under non-templated conditions at the concentrations used. Obviously, the reaction only proceeded in the presence of a complementary template strand. When using the template 29mer-r (see Figure 5b), which contains the complementary 14mer-sequences in a reversed manner, we did not observe any reaction, either (Figure S3). This is an expected result as, with this template, hybridization positions the dienophile and tetrazine distant from each other, not able to meet for reaction.

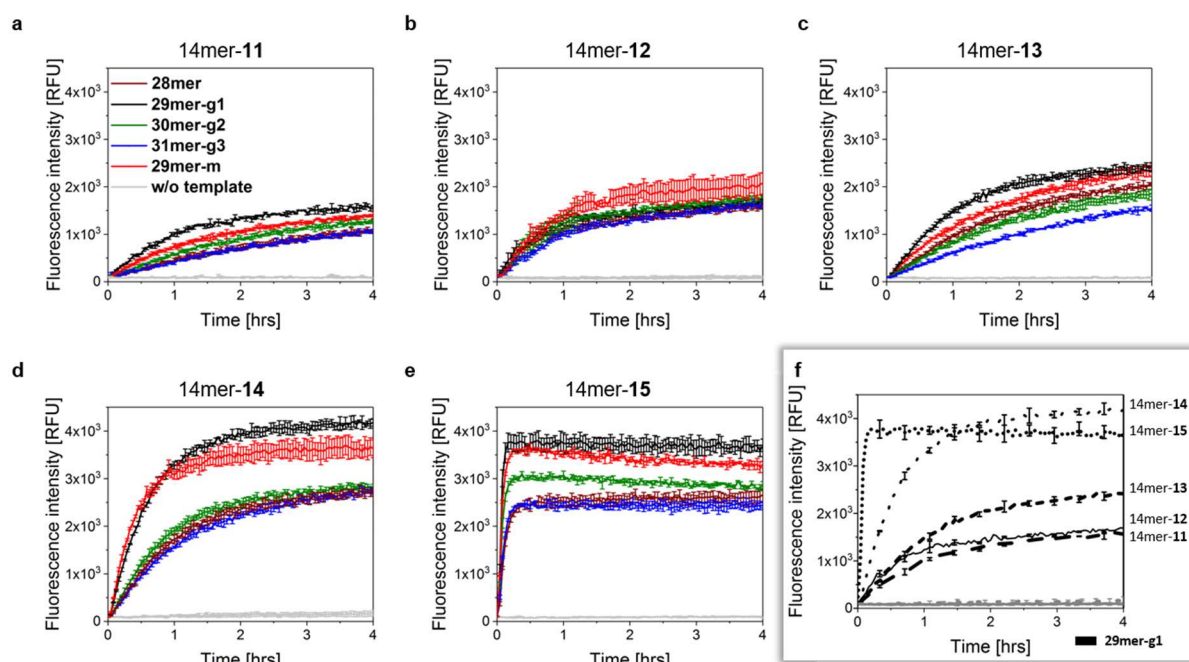


Figure 6: Kinetics of template-mediated DA_{inv} between 14mer-**dienophiles** and 14mer-**Rhod-Tz**. (a-e) Using various template sequences for the 14mer-**dienophiles**. (f) Comparison of all 14mer-**dienophiles** in proximity-induced DA_{inv} using template 29mer-**g1**. Both reactants and templates were used in equimolar quantities in PBS (1 μ M).

The template-mediated DA_{inv} with the templates 28mer, 29mer-**g1**, 30mer-**g2**, 31mer-**g3** in all cases showed strong rate enhancement over the non-templated reaction (Figure 6a-e). While the fastest kinetics can be observed with the **g1**-template, the **g2**- and **g3**-template showed the expected slower kinetics, due to the increasing distance between dienophile and tetrazine. This trend is consistent for all dienophiles used in the study and is in accordance with other DNA-templated proximity systems reported in literature,^[24a] where a single nucleotide gap has also been shown to be favorable. The 28mer-template, which theoretically leads to the closest positioning of both reactants, clearly showed slower reaction kinetics than the 29mer-**g1**-template. This observation might result from the type of modification we chose for the attachment of the reactants to the 5'- and 3'-position of the respective 14mers (see Figure S1). The modification of the 14mer at the 5'-phosphate with the dienophile respectively at the 3'-hydroxy with the tetrazine can lead to sterically disfavored reactant orientation when used with the 28mer template. This indicates the importance of spatial orientation of reactants for the probability of collision, a prerequisite for reaction. Interestingly, we also see differences in the total change of fluorescence over time for the different templates while using the same 14mer-**dienophile** and 14mer-**Rhod-Tz**. Although this effect is not dramatic, the differences are clearly visible from the fluorescence after completion of the reaction. It should be noted that the formed Diels-Alder product is identical in each experiment, though hybridized to

different template strands. The hybridization of the ligated 14mer-strands to the different templates might lead to differences in the degrees of freedom for the formed fluorescent cycloadduct, resulting in slightly different fluorescence properties. Figure 6f summarizes the reaction kinetics of all five 14mer-**dienophiles** in the presence of the 29mer-**g1** template. The dienophiles that are more reactive in DA_{inv} also show faster kinetics in the proximity-induced reaction. Again we observed different fluorescence intensities after full conversion. However, the differences of the fluorescence intensities were significantly higher compared to the previous results when only the template sequence was variable. It has to be noted that the formed Diels-Alder products in Figure 6f are different, which is likely to result in fluorophores with different quantum yields. This has previously been described for fluorogenic tetrazine conjugated probes.^[29c] Moreover, DA_{inv} between tetrazines and olefins results in a mixture of tautomeric and diastereomeric dihydropyridazines as well as pyridazines.^[7a, 7b, 33] We found the strongest fluorescence increase after full conversion to be 42-fold for the dienophile 14mer-**14**. Full conversion of the ligation process (indicated by reaching a plateau) was verified and analyzed by ESI-TOF HRMS and no side products could be identified. Furthermore, we analyzed the aqueous stability (PBS, pH 7.4, 30°C) of the oligonucleotide fluorogenic tetrazine rhodamine conjugate by HR-MS and HPLC, which was found to be stable with no significant degradation of the tetrazine moiety for at least 12 hours.

As expected, the fastest reaction was observed with 14mer-**15** reaching the maximum fluorescence after six minutes. 14mer-**14** showed the second highest reactivity and the respective DA_{inv} -product possessed the highest observed turn-on value (Figure 6f). Additionally, we analyzed the influence on the reaction kinetics when using a template with a single mismatch in the sequence (29mer-**m**) (Figure 4c). The mismatch, three bases apart from the ligation site, caused a deceleration of the DA_{inv} compared to the gap-template 29mer-**g1**. Apparently, the introduced mismatch led to a slightly delayed reaction, likely due to a perturbed hybridization process. However, the effect of the mismatch on the reaction rate was less pronounced compared to templates 30mer-**g2** or 31mer-**g3**.

An overview of the above-noted maximal fluorescence turn-on values of templated DA_{inv} is shown in Figure 7a. The fold increases were calculated by dividing the final fluorescence intensity by the respective baseline intensities. The lowest turn-on values were obtained for the primary alkenes 14mer-**11** and 14mer-**12** (7 to 19-fold). 14mer-**13** and 14mer-**15** exhibited

turn-on values between 24 and 35-fold. The highest fluorescence increase was determined to 42-fold for the 29mer-g1-templated reaction of 14mer-14.

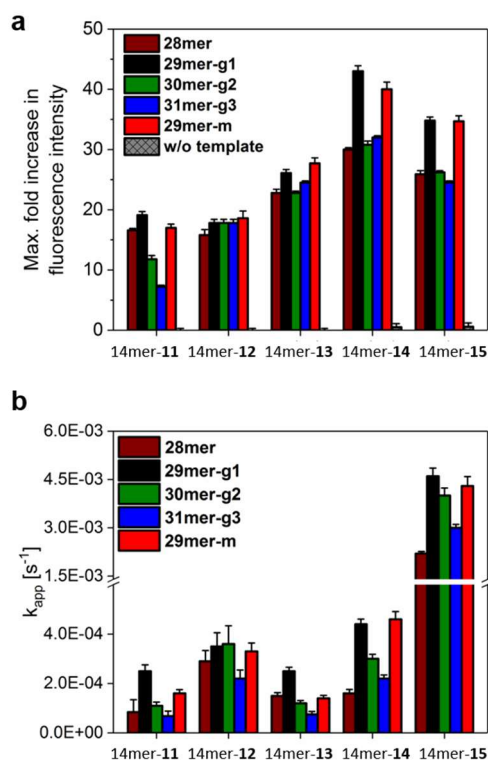


Figure 7: (a) Fluorescence fold increase after reaction completion in proximity-induced DA_{inv} (up to 43-fold). (b) Overview of calculated apparent first-order rate constants k_{app} (spanning almost two orders of magnitude).

To determine the apparent first-order rate constants (k_{app}) from the reaction kinetics, an exponential function was applied to the measured fluorescence data. The obtained data is summarized in Figure 7b and Table S3. The lowest k_{app} were determined for primary olefin 14mer-11 (k_{app} [$10^{-4} s^{-1}$] = [0.7±0.2] to [2.5±0.3]) and cyclopentene 14mer-13 (k_{app} [$10^{-4} s^{-1}$] = [0.8±0.1] to [2.5±0.2]). Interestingly, the rates of primary olefin 14mer-12 (k_{app} [$10^{-4} s^{-1}$] = [2.2±0.3] to [3.6±0.7]) were higher than those of cyclopentene 14mer-13 and were of the same order of magnitude as cyclopentene 14mer-14 (k_{app} [$10^{-4} s^{-1}$] = [1.6±0.2] to [4.6±0.3]). Two major factors have to be taken into account here: First, the electron densities of the alkenes differ depending on the position of the amide group. Secondly, length and conformational flexibility of the reactants influence the probability for a collision that leads to a chemical reaction. The longer carbon chain in nonenoic acid of 14mer-12 might have played a role for the increased reaction rate compared to 14mer-11 and 14mer-13 and the increased dienophile flexibility surpassed the higher reactivity in DA_{inv} of cyclopentene derivatives. The higher rate of the cyclopentene moiety in 14mer-14 compared to the one in 14mer-13 could

arise from the higher dienophile-mobility and lower electron deficiency (α -dialkyl-substituted alkene) in 14mer-**14**. Expectedly, k_{app} significantly increased for norbornene 14mer-**15**, the most reactive dienophile used in this study, to the highest herein determined values ($k_{app} [10^{-4} \text{ s}^{-1}] = [22 \pm 1] \text{ to } [46 \pm 3]$). The determined k_{app} are in accordance with reported first-order rate constants for DNA-templated reactions.^[21b, 24, 34] The half-lives ranged from 46 ± 6 min (14mer-**11**) to 2.5 ± 0.9 min (14mer-**15**) in DA_{inv} with 29mer-**g1** as template (Table S4). Taken together, the kinetic analysis illustrates the considerable extent to which reaction rates differ from non-templated DA_{inv} -conditions (see above, negligible to 0.6% conversion) to templated conditions. Under proximity-induced acceleration, the dienophile-reactivity as well as mobility and length of linker structures greatly influence the reaction rate. Moreover, the choice of the template (fully complementary, gap length at DA_{inv} -site) results in varying reaction rates. The template-length and linker structure-dependency of the reaction kinetics are in accordance with previous reports.^[15a, 24a] Still, the reactivity of the dienophile was the determining factor for the reaction rates observed in the template-mediated DA_{inv} .

In summary, the kinetics of dienophiles were investigated in terms of their performance in DA_{inv} using a templated model system. Stable dienophiles with poor kinetic characteristics did not react at micromolar concentrations without a DNA template strand present. However, the hybridization-induced reactions between the tetrazine probe and dienophiles were significantly accelerated and k_{app} ranging from 10^{-3} to 10^{-4} s^{-1} were determined. Remarkably, the templated fluorogenic bioorthogonal reaction led to an increase in fluorescence intensity of up to 42 ± 1 -fold. This observed fluorescence turn-on was higher compared to the reaction between **Rhod-Tz** and BCN (34 ± 2 -fold). The reason for this could be environmental effects of the oligonucleotides in addition to different quantum yields of the formed cycloadducts. Furthermore, we suggest the use of cyclopentene derivative **14** in future fluorogenic proximity-enhanced biorthogonal experiments. It equates to a minimal sized tag and, as our study shows, it combines reasonable kinetics with a high fluorescence turn-on (42-fold).

Conclusion

In this work we report the effect of proximity on DA_{inv} -biorthogonal chemistry by evaluating dienophiles of varying reactivity in a well-defined DNA-templated assay. We developed a highly convergent, modular synthesis route towards easily modifiable multi-functional fluorogenic xanthene-based dyes ready for bioconjugation. The synthetic route provides

access to future tailor-made probes through simple modification of the used building blocks. The synthesized probe **Rhod-Tz-NHS** represents the first fluorogenic tetrazine crosslinker based on a rhodamine fluorophore. For the purpose of this study, the novel bifunctional tetrazine-dye served us as fluorescence turn-on probe, providing us the direct read-out necessary to study different dienophiles in proximity-induced bioorthogonal DA_{inv}. Our study shows that the lack in reactivity in DA_{inv} of highly stable dienophiles with poor kinetic characteristics can be overcome by DNA-templated chemistry induced proximity. Fluorescence signal generation resulted solely from proximity-induced reaction, while background reactivity was absent at micromolar concentrations. The concept of proximity can be highly beneficial to overcome stability problems of commonly used reactants in bioorthogonal chemistry while maintaining the rapid reaction rates needed for cellular applications. Furthermore, the results indicate the potential of our fluorogenic tetrazine dye **Rhod-Tz** for the visualization of biomolecular interactions with temporal and spatial resolution *in vitro* as well as in living systems.

Acknowledgements

R.W. acknowledges funding from the Deutsche Forschungsgemeinschaft DFG (SPP1623, WO 1888/1-2). We thank Dr. Achim Wieczorek for scientific advice, Mathis Baalman and Michael Ziegler for helpful comments to the manuscript. We gratefully acknowledge Prof. Dr. Andres Jäschke for constant support.

References

- [1] B. M. Trost, T. N. Salzman, *J. Am. Chem. Soc.* **1973**, *95*, 6840-6842.
- [2] P. Müller, *Pure Appl. Chem.* **1994**, *66*, 1097.
- [3] H. C. Hang, C. Yu, D. L. Kato, C. R. Bertozzi, *Proc. Natl. Acad. Sci. U. S. A.* **2003**, *100*, 14846-14851.
- [4] E. M. Sletten, C. R. Bertozzi, *Angew. Chem., Int. Ed.* **2009**, *48*, 6974-6998.
- [5] E. Saxon, C. R. Bertozzi, *Science* **2000**, *287*, 2007-2010.
- [6] N. J. Agard, J. A. Prescher, C. R. Bertozzi, *J. Am. Chem. Soc.* **2004**, *126*, 15046-15047.
- [7] a) M. L. Blackman, M. Royzen, J. M. Fox, *J. Am. Chem. Soc.* **2008**, *130*, 13518-13519; b) N. K. Devaraj, R. Weissleder, S. A. Hilderbrand, *Bioconjugate Chem.* **2008**, *19*, 2297-2299; c) R. Pipkorn, W. Waldeck, B. Didinger, M. Koch, G. Mueller, M. Wiessler, K. Braun, *J. Pept. Sci.* **2009**, *15*, 235-241.
- [8] a) B. L. Oliveira, Z. Guo, G. J. L. Bernardes, *Chem. Soc. Rev.* **2017**, DOI: 10.1039/C1037CS00184C; b) S. Mayer, K. Lang, *Synthesis* **2017**, *49*, 830-848; c) E. Kozma, O. Demeter, P. Kele, *ChemBioChem* **2017**, *18*, 486-501.
- [9] A. Darko, S. Wallace, O. Dmitrenko, M. M. Machovina, R. A. Mehl, J. W. Chin, J. M. Fox, *Chem. Sci.* **2014**, *5*, 3770-3776.

- [10] a) D. C. Rideout, R. Breslow, *J. Am. Chem. Soc.* **1980**, *102*, 7816-7817; b) M. C. Pirrung, K. D. Sarma, *J. Am. Chem. Soc.* **2004**, *126*, 444-445.
- [11] a) R. Rossin, S. M. van den Bosch, W. ten Hoeve, M. Carvelli, R. M. Versteegen, J. Lub, M. S. Robillard, *Bioconjugate Chem.* **2013**, *24*, 1210-1217; b) M. Best, A. Degen, M. Baalman, T. T. Schmidt, R. Wombacher, *ChemBioChem* **2015**, *16*, 1158-1162.
- [12] a) R. M. Versteegen, R. Rossin, W. ten Hoeve, H. M. Janssen, M. S. Robillard, *Angew. Chem., Int. Ed.* **2013**, *52*, 14112-14116; b) J. Li, S. Jia, P. R. Chen, *Nat. Chem. Biol.* **2014**, *10*, 1003-1005.
- [13] a) T. Kämpchen, W. Massa, W. Overheu, R. Schmidt, G. Seitz, *Chem. Ber.* **1982**, *115*, 683-694; b) M. R. Karver, R. Weissleder, S. A. Hilderbrand, *Bioconjugate Chem.* **2011**, *22*, 2263-2270.
- [14] a) M. T. Taylor, M. L. Blackman, O. Dmitrenko, J. M. Fox, *J. Am. Chem. Soc.* **2011**, *133*, 9646-9649; b) K. Tomooka, S. Miyasaka, S. Motomura, K. Igawa, *Chem. Eur. J.* **2014**, *20*, 7598-7602; c) I. Nikić, T. Plass, O. Schraidt, J. Szymański, J. A. G. Briggs, C. Schultz, E. A. Lemke, *Angew. Chem., Int. Ed.* **2014**, *53*, 2245-2249; d) H. E. Murrey, J. C. Judkins, C. W. am Ende, T. E. Ballard, Y. Fang, K. Riccardi, L. Di, E. R. Guilmette, J. W. Schwartz, J. M. Fox, D. S. Johnson, *J. Am. Chem. Soc.* **2015**, *137*, 11461-11475; e) J. Santucci, J. R. Sanzone, K. A. Woerpel, *Eur. J. Org. Chem.* **2016**, *2016*, 2933-2943; f) E. Kozma, I. Nikić, B. R. Varga, I. V. Aramburu, J. H. Kang, O. T. Fackler, E. A. Lemke, P. Kele, *ChemBioChem* **2016**, *17*, 1518-1524; g) W. D. Lambert, S. L. Scinto, O. Dmitrenko, S. J. Boyd, R. Magboo, R. A. Mehl, J. W. Chin, J. M. Fox, S. Wallace, *Org. Biomol. Chem.* **2017**, DOI: 10.1039/C1037OB01707C.
- [15] a) A. P. Silverman, E. T. Kool, *Chem. Rev.* **2006**, *106*, 3775-3789; b) K. Gorska, N. Winssinger, *Angew. Chem., Int. Ed.* **2013**, *52*, 6820-6843; c) M. Di Pisa, O. Seitz, *ChemMedChem* **2017**, *12*, 872-882.
- [16] a) J. Cai, X. Li, X. Yue, J. S. Taylor, *J. Am. Chem. Soc.* **2004**, *126*, 16324-16325; b) Z. L. Pianowski, N. Winssinger, *Chem. Commun.* **2007**, 3820-3822; c) H. Abe, J. Wang, K. Furukawa, K. Oki, M. Uda, S. Tsuneda, Y. Ito, *Bioconjugate Chem.* **2008**, *19*, 1219-1226; d) R. M. Franzini, E. T. Kool, *J. Am. Chem. Soc.* **2009**, *131*, 16021-16023; e) Z. Pianowski, K. Gorska, L. Oswald, C. A. Merten, N. Winssinger, *J. Am. Chem. Soc.* **2009**, *131*, 6492-6497; f) R. M. Franzini, E. T. Kool, *Bioconjugate Chem.* **2011**, *22*, 1869-1877; g) R. M. Franzini, E. T. Kool, *Chem. Eur. J.* **2011**, *17*, 2168-2175; h) K. Furukawa, H. Abe, Y. Tamura, R. Yoshimoto, M. Yoshida, S. Tsuneda, Y. Ito, *Angew. Chem., Int. Ed.* **2011**, *50*, 12020-12023.
- [17] a) R. Kumar, A. El-Sagheer, J. Tumpene, P. Lincoln, L. M. Wilhelmsson, T. Brown, *J. Am. Chem. Soc.* **2007**, *129*, 6859-6864; b) M. Shelbourne, X. Chen, T. Brown, A. H. El-Sagheer, *Chem. Commun.* **2011**, *47*, 6257-6259.
- [18] a) S. Ficht, A. Mattes, O. Seitz, *J. Am. Chem. Soc.* **2004**, *126*, 9970-9981; b) T. N. Grossmann, O. Seitz, *J. Am. Chem. Soc.* **2006**, *128*, 15596-15597; c) E. Jentsch, A. Mokhir, *Inorg. Chem.* **2009**, *48*, 9593-9595; d) D. Chouikhi, S. Barluenga, N. Winssinger, *Chem. Commun.* **2010**, *46*, 5476-5478; e) A. Roloff, O. Seitz, *Chem. Sci.* **2013**, *4*, 432-436.
- [19] a) Y. Xu, N. B. Karalkar, E. T. Kool, *Nat. Biotechnol.* **2001**, *19*, 148-152; b) G. P. Miller, A. P. Silverman, E. T. Kool, *Bioorg. Med. Chem.* **2008**, *16*, 56-64.
- [20] a) J. Liu, J.-S. Taylor, *Nucleic Acids Res.* **1998**, *26*, 3300-3304; b) K. Fujimoto, S. Matsuda, N. Takahashi, I. Saito, *J. Am. Chem. Soc.* **2000**, *122*, 5646-5647; c) M. Röthlingshöfer, K. Gorska, N. Winssinger, *Org. Lett.* **2012**, *14*, 482-485.

- [21] a) W. A. Velema, E. T. Kool, *J. Am. Chem. Soc.* **2017**, *139*, 5405-5411; b) D. Chang, E. Lindberg, N. Winssinger, *J. Am. Chem. Soc.* **2017**, *139*, 1444-1447.
- [22] a) J. Singh, R. C. Petter, T. A. Baillie, A. Whitty, *Nat. Rev. Drug Discov.* **2011**, *10*, 307-317; b) R. Lagoutte, R. Patouret, N. Winssinger, *Curr. Opin. Chem. Biol.* **2017**, *39*, 54-63; c) M. J. C. Long, Y. Aye, *Cell Chem. Biol.* **2017**.
- [23] a) M. Sunbul, L. Nacheva, A. Jäschke, *Bioconjugate Chem.* **2015**, *26*, 1466-1469; b) Z. Chen, C. Jing, S. S. Gallagher, M. P. Sheetz, V. W. Cornish, *J. Am. Chem. Soc.* **2012**, *134*, 13692-13699; c) Y. Takaoka, Y. Nishikawa, Y. Hashimoto, K. Sasaki, I. Hamachi, *Chem. Sci.* **2015**, *6*, 3217-3224; d) T. Tamura, Y. Kioi, T. Miki, S. Tsukiji, I. Hamachi, *J. Am. Chem. Soc.* **2013**, *135*, 6782-6785; e) S. Tsukiji, I. Hamachi, *Curr. Opin. Chem. Biol.* **2014**, *21*, 136-143.
- [24] a) J. Šečkutė, J. Yang, N. K. Devaraj, *Nucleic Acids Res.* **2013**, *41*, e148-e148; b) H. Wu, B. T. Cisneros, C. M. Cole, N. K. Devaraj, *J. Am. Chem. Soc.* **2014**, *136*, 17942-17945; c) H. Wu, S. C. Alexander, S. Jin, N. K. Devaraj, *J. Am. Chem. Soc.* **2016**, *138*, 11429-11432.
- [25] A. Wieczorek, P. Werther, J. Euchner, R. Wombacher, *Chem. Sci.* **2017**, *8*, 1506-1510.
- [26] a) A. V. Anzalone, T. Y. Wang, Z. Chen, V. W. Cornish, *Angew. Chem., Int. Ed.* **2013**, *52*, 650-654; b) D. Maiti, S. L. Buchwald, *J. Am. Chem. Soc.* **2009**, *131*, 17423-17429.
- [27] A. Klapars, S. L. Buchwald, *J. Am. Chem. Soc.* **2002**, *124*, 14844-14845.
- [28] a) D.-S. Mei, Y. Qu, J.-X. He, L. Chen, Z.-J. Yao, *Tetrahedron* **2011**, *67*, 2251-2259; b) J. N. N. Eildal, A. Bach, J. Dogan, F. Ye, M. Zhang, P. Jemth, K. Strømgaard, *ChemBioChem* **2015**, *16*, 64-69.
- [29] a) J. C. T. Carlson, L. G. Meimetis, S. A. Hilderbrand, R. Weissleder, *Angew. Chem., Int. Ed.* **2013**, *52*, 6917-6920; b) L. G. Meimetis, J. C. T. Carlson, R. J. Giedt, R. H. Kohler, R. Weissleder, *Angew. Chem., Int. Ed.* **2014**, *53*, 7531-7534; c) H. Wu, J. Yang, J. Šečkutė, N. K. Devaraj, *Angew. Chem., Int. Ed.* **2014**, *126*, 5915-5919; d) G. Knorr, E. Kozma, A. Herner, E. A. Lemke, P. Kele, *Chem. Eur. J.* **2016**, *22*, 8972-8979; e) A. Wieczorek, T. Buckup, R. Wombacher, *Org. Biomol. Chem.* **2014**, *12*, 4177-4185.
- [30] a) A. Niederwieser, A.-K. Späte, L. D. Nguyen, C. Jüngst, W. Reutter, V. Wittmann, *Angew. Chem., Int. Ed.* **2013**, *52*, 4265-4268; b) Y.-J. Lee, Y. Kurra, Y. Yang, J. Torres-Kolbus, A. Deiters, W. R. Liu, *Chem. Commun.* **2014**, *50*, 13085-13088; c) B. L. Oliveira, Z. Guo, O. Boutureira, A. Guerreiro, G. Jiménez-Osés, G. J. L. Bernardes, *Angew. Chem., Int. Ed.* **2016**, *55*, 14683-14687; d) U. Rieder, N. W. Luedtke, *Angew. Chem., Int. Ed.* **2014**, *126*, 9322-9326; e) X. Shang, X. Song, C. Faller, R. Lai, H. Li, R. Cerny, W. Niu, J. Guo, *Chem. Sci.* **2017**, *8*, 1141-1145.
- [31] a) J. Yang, J. Šečkutė, C. M. Cole, N. K. Devaraj, *Angew. Chem., Int. Ed.* **2012**, *51*, 7476-7479; b) D. M. Patterson, L. A. Nazarova, B. Xie, D. N. Kamber, J. A. Prescher, *J. Am. Chem. Soc.* **2012**, *134*, 18638-18643.
- [32] C. Uttamapinant, J. D. Howe, K. Lang, V. Beránek, L. Davis, M. Mahesh, N. P. Barry, J. W. Chin, *J. Am. Chem. Soc.* **2015**, *137*, 4602-4605.
- [33] J. Schoch, M. Wiessler, A. Jäschke, *J. Am. Chem. Soc.* **2010**, *132*, 8846-8847.
- [34] A. Shibata, T. Uzawa, Y. Nakashima, M. Ito, Y. Nakano, S. Shuto, Y. Ito, H. Abe, *J. Am. Chem. Soc.* **2013**, *135*, 14172-14178.